

A simple model to compute the blood flows through obstructed blood vessels

Mohsen Gh Kharaji¹, Fakhroddin Dadjoo², Y Alirezaei³, Ali Falavand⁴, Ameneh Langari*⁵

¹Shahrekord University of Medical Sciences, Shahrekord, Iran

²Civil Engineering Group, Chaloos Branch, Islamic Azad University, Chaloos, Iran

³Engineering Group, Cirjan Branch, Islamic Azad University, Cirjan, Iran

⁴Engineering Group, Ahvaz Branch, Islamic Azad University, Ahvaz, Iran

⁵North Khorasan University of Medical Sciences, Bojnurd, Iran

Corresponding author email: amenehlangari@yahoo.com

Abstract: The aim of this article is to measuring the blood flow, when they pass through obstructed blood vessels. In many medical arteries the amount of the blood flow inside canals and obstructed vessel is important and reduces due to the arteries. However, the problem with measurements in such circumstances lies in the lack of precise and appropriate experimental data needed for the calculation of the blood passes through the vessel. To overcome the shortcoming, hence, the effect of the most common type orifices, i.e., Square edge Orifice (D & $D/2$ taps), were put to the test, by simulating the flow with the use of CFD methods and Fluent 6.0 software, for $0.25 \leq \beta \leq 0.5$ and $10,000 \leq Re_D \leq 200,000$, fixed temperature of 300^K . Therefore, relations were obtained for blood as the incompressible fluid.

[Kharaji M. Gh., Dadjoo F., Alirezaei Y., Falavand A., Langari A. **A simple model to compute the blood flows through obstructed blood vessels.** *Life Sci J* 2012;9(4):1782-1788] (ISSN:1097-8135). <http://www.lifesciencesite.com>. 271

Keywords: Blood flow, Orifice, Vessel, Fluent, Computational fluid dynamic (CFD)

1. Introduction

Disruption of normal blood flow to the heart, lung, and brain due to thrombosis is one of the leading causes of death and long-term adult disability in the developing world. Today, patients with pulmonary embolism, strokes, heart attacks and other types of acute thrombosis leading to near-complete vascular occlusion are most frequently treated in an acute care hospital setting using systemic dosages of powerful clot-dissolving drugs [1].

The obstructed part of the vessel can be simulated through an orifice. Orifice can be simulated as a plate with a hole in the middle which is vertical to the fluid. When the fluid reaches the orifice with a constant velocity and pressure, it has to be contracted in order to pass through the orifice hole. The maximum point of this contraction is called the “*Vena Contracta (VC)*” point which is actually placed after the orifice.

The pressure and velocity of the blood flow will change, while passing through the V.C. point and after that the fluid will once again expand and the pressure and velocity will again change.

By calculating the differences in pressure and velocity, we can calculate the flow of fluid with the help of Bernoulli equation. The sizing error factor is assigned by the ANSA/API 2530 standard.

The contraction form which happens after the orifice will make the results of the calculations using the Bernoulli equation, different to the ones determined by experiments; therefore a correction

factor must be determined in order to lower the error. This factor is called the “*discharge coefficient*” factor, and is usually calculated experimentally for different orifices with different β ratios.

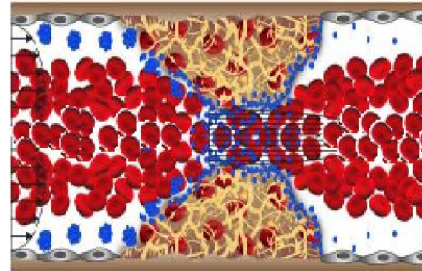


Figure 1. Blood flow through a obstructed vessel.

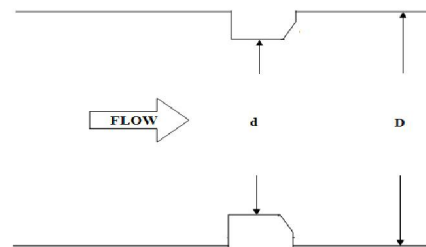


Figure 2. Square edge concentric orifice, with sizing parameters

The results of these calculations are available in reference books as charts, but it is not general and only available for particular conditions.

The biggest problem is that these experiments have been widely done for compressible and incompressible fluids, and there is not much data available for two phase fluids and this lack of information has caused many problems.

Therefore, the aim of this project is to determine a new formula which can predict the discharge coefficient for the incompressible fluids at the β ratios between 0.25 and 0.5, with a standard error of 4-5 percent. After that some relations will be given for compressible and also two phase fluids which are widely used in the oil and gas industries. We hope to decrease the lack of information in this part and help them.

2. Theoretical basis

To control industrial processes, it is essential to know the amount of material entering and leaving the process. A few types of flow meters measure the mass flow rate directly, but the majority measures the volumetric flow rate or the average fluid velocity, from which the volumetric flow rate can be calculated. Most meters operate on all the fluid in the pipe or channel and are known as *full-bore meters*. Others, called *insertion meters*, measure the flow rate, or more commonly the fluid velocity, at one point only. The total flow rate, however, can often be inferred with considerable accuracy from this single-point measurement.

The most common types of full-bore meters are Venturi and Orifice meters.

A Venturi meter is a short conical inlet section leads to a throat section, then to a long discharge cone. Although Venturi meters can be applied to the measurement of gas flow rates, they are most commonly used with liquids, especially large flows of liquids where, because of the large pressure recovery, a Venturi requires less power than other types of meters.

The Venturi meter has certain practical disadvantages for ordinary plant practice. It is expensive, it occupies considerable space, and its ratio of throat diameter to pipe diameter can not be changed. For a given meter and definite manometer system, the maximum measurable flow rate is fixed, so if the flow range is changed, the throat diameter may be too large to give an accurate reading or too small to accommodate the next maximum flow rate. The orifice meter meets these objections to the Venturi but at the price of large power consumption.

In 2-in (50 mm) and larger line sizes the concentric orifice (Figure 2) is the most common restriction for clean liquids, gases, and low-velocity vapor (steam) flows. It is a sharp, square-edge hole bored in a flat, thin plate. The ratio of opening diameter d to pipe diameter D defines the β ratio. For

most applications this ratio should be between 0.2 and 0.75, depending on desired differential; a high β orifice produces less differential for the same flow rate than a small β orifice.

Depending on upstream and downstream tap locations, the flow meter is referred to as a corner tap, a flange tap, a D-and-D/2 tap, a pipe tap (2.5 D and 8D), or a vena contracta tap orifice flow meter. Vena contracta taps have been replaced by D-and-D/2 taps because future changes in orifice bore require no tap relocation.

Several standards [2,3] have been written to detail installation requirements and construction and to estimate the overall uncertainty (accuracy) [3].

The maximum pipe Reynolds number may be as high as 3.3×10^7 . However, a discharge coefficient rise of up to 1.56 percent for a 0.71 β ratio orifice has been reported by Jones at bore Reynolds number greater than 8×10^6 . This rise, may be explained by the work of Grose on the inviscid (zero viscosity) contraction coefficient change with β ratio.

The basic equation for an orifice meter is obtained by writing the Euler equation for incompressible fluids across the upstream [4]:

$$\rho \left(\frac{\partial u}{\partial t} + u \frac{\partial u}{\partial x} + v \frac{\partial u}{\partial y} + w \frac{\partial u}{\partial z} \right) = -\frac{\partial p}{\partial x} + \rho g_x \quad (1)$$

$$v, w = 0$$

$$\rho u \left(\frac{\partial u}{\partial t} + u \frac{\partial u}{\partial x} \right) = -u \frac{\partial p}{\partial x} + \rho u g_x \quad (2)$$

Or

$$\rho \left[\frac{\partial(u^2/2)}{\partial t} + u \frac{\partial(u^2/2)}{\partial x} \right] = -u \frac{\partial p}{\partial x} + \rho u g_x \quad (3)$$

Since flow is steady, the left-hand term in equation (1) vanishes. There is no variation in fluid velocity across the cross section, so the flow is unidirectional and the velocity u is a function only of x and since gravity acts in the negative x direction, $g_x = -g$. The partial differentials become total differentials. Hence, from equation (1),

$$u \frac{d(\rho u^2/2)}{dx} + u \frac{dp}{dx} + \rho u g = 0 \quad (4)$$

Thus for steady flow it is possible to divide through by the velocity u . by doing this and also dividing through by ρ equation (2) becomes:

$$\frac{d(u^2/2)}{dx} + \frac{1}{\rho} \frac{dp}{dx} + g \frac{dZ}{dx} = 0 \quad (5)$$

In a straight horizontal tube, in consequences, there is *no* pressure drop in steady constant-velocity potential flow. Integrating equation (3) will give:

$$\frac{P_a}{\rho} + gZ_a + \frac{u_a^2}{2} = \frac{P_b}{\rho} + gZ_b + \frac{u_b^2}{2} \quad (6)$$

Equation (4) is known as the Bernoulli equation without friction.

Most fluid flow problems encountered in engineering involve streams that are influenced by solid boundaries and therefore contain boundary layers. This is especially true in the flow of fluids through pipes and other equipments, where the entire stream may be in boundary layer flow.

To extend the Bernoulli equation to cover practical situations, two modifications are needed. The first, usually of minor importance, is a correction of the kinetic energy term for the variation of local velocity u with position in the boundary layer; the second, of major importance, is the correction of equation for the existence of fluid friction, which appears when ever a boundary layer forms.

The term $u^2/2$ in equation (4) is the kinetic energy of a unit mass of fluid all of which is flowing at the same velocity u . when the velocity varies across the stream cross section, the kinetic energy is found in the following manner. Consider an element of cross-sectional area dS . The mass flow rate through this is $\rho u dS$. Each and the energy flow rate through area dS carries kinetic energy in amount $u^2/2$, and the energy flow rate through area dS is therefore:

$$d\dot{E}_k = (\rho u dS) \frac{u^2}{2} = \frac{\rho u^3 dS}{2} \quad (7)$$

Where \dot{E}_k represents the time rate of flow of kinetic energy. The total rate of flow of kinetic energy through the entire cross section S is, assuming constant density within the area S ,

$$\dot{E}_k = \frac{\rho}{2} \int_S u^3 dS \quad (8)$$

Then

$$\frac{\dot{E}_k}{\dot{m}} = \frac{\frac{1}{2} \int_S u^3 dS}{\int_S u dS} = \frac{\frac{1}{2} \int_S u^3 dS}{\bar{V} S} \quad (9)$$

2.1 Kinetic energy correction factor

It is convenient to eliminate the integral of equation (5) by a factor operating on $\frac{\bar{V}^2}{2}$ to give the correct value of the kinetic energy. This factor, called the kinetic energy correction factor, is denoted by α and is defined by

$$\frac{\alpha \bar{V}^2}{2} = \frac{\dot{E}_k}{\dot{m}} = \frac{\int_S u^3 dS}{2 \bar{V} S} \quad (10)$$

$$\alpha = \frac{\int_S u^3 dS}{\bar{V}^3 S}$$

2.2 Correction of Bernoulli equation for fluid friction

Friction manifests itself by the disappearance of mechanical energy. In frictional flow the quantity

$$\frac{p}{\rho} + \frac{u^2}{2} + gZ \quad (11)$$

is not constant along streamline, as called for by equation (4), but always decreases in the direction of flow.

For incompressible fluids, the Bernoulli equation is corrected for friction by adding a term to the right-hand side of equation (4). Thus, after introducing the kinetic energy correction factor, equation (4) becomes

$$\frac{P_a}{\rho} + gZ_a + \frac{\alpha_a \bar{V}_a^2}{2} = \frac{P_b}{\rho} + gZ_b + \frac{\alpha_b \bar{V}_b^2}{2} + h_f \quad (12)$$

If \bar{V}_a and \bar{V}_b are the average upstream and downstream velocities, respectively, and ρ is the density of the fluid, equation (7) becomes

$$\alpha_b \bar{V}_b^2 - \alpha_a \bar{V}_a^2 = \frac{2(p_a - p_b)}{\rho} \quad (13)$$

$$\bar{V}_a = \left(\frac{D_b}{D_a} \right)^2 \bar{V}_b = \beta^2 \bar{V}_b \quad (14)$$

If \bar{V}_a is eliminated from equations (8) and (9), the result is

$$\bar{V}_b = \frac{1}{\sqrt{\alpha_b - \beta^4 \alpha_a}} \sqrt{\frac{2(p_a - p_b)}{\rho}} \quad (15)$$

Equation (10) applies strictly to the frictionless flow of noncompressible fluids. To calculate the mass flow rate

$$Q = \rho \bar{V} A \quad (16)$$

Therefore

$$Q = \frac{\pi}{4} \frac{D_a^2}{\sqrt{\alpha_b - \beta^4 \alpha_a}} \sqrt{\frac{2(p_a - p_b)}{\rho}} \quad (17)$$

2.3 Correction to the theoretical equation:

The theoretical flow equation calculates the true flow rate only when all the assumptions used to

develop it are valid. This is seldom the case, and the true flow rate is almost always less than the theoretically calculated value.

How closely the true flow rate can be calculated depends almost entirely on the geometry of the contraction. For a venturi or flow nozzle, where the area reduction is gradual the agreement is within 1 to 3 percent. But for the square-edge orifice the abrupt area reduction places the minimum flow area downstream of the plane of the vena contracta. Since the diameter of the vena contracts (D_{VC}) for an orifice cannot be measured, the theoretical equation includes the measured bore as the correlation diameter. Also, increased downstream turbulence results in an energy loss that is not accounted for by either Bernoulli's equation or the thermodynamic steady flow energy equation. These two factors result in the true flow being approximately 60 percent of the theoretically calculated value. The location of the two measuring taps is also important because it establishes the measured differential.

The theoretical equation is adjusted for these effects with two empirically determined corrections. The first is the *discharge coefficient* C , which corrects for velocity profile (Reynolds number), tap location, and contraction geometry; the second is an empirically derived *net expansion-factor equation* for orifice flow meters.

2.4 Discharge Coefficient

For a given primary element, the discharge coefficient is derived from laboratory data by rotating the true and theoretical flow rates. The true flow rate is determined by weighing or volumetric collection of the fluid over a measured time interval, and the theoretical flow rate is calculated with equation (11). The discharge coefficient is then defined as

$$C = \frac{\text{true flow rate}}{\text{theoretical flow rate}} \quad (18)$$

The discharge coefficient corrects the theoretical equation for the influences of velocity profile (Reynolds number), the assumption of no energy loss between taps, and pressure-tap location.

In some flow equations, the discharge coefficient is combined with velocity of approach and redefined as the *flow coefficient*. For fixed geometry primary devices, to simplify the equation, or where primary elements are available in a limited range of sizes, the flow coefficient is used in place of the discharge coefficient. The flow coefficient is defined as

$$K = \frac{C}{\sqrt{1-\beta^4}} = EC \quad (19)$$

Where E is the velocity of approach factor [5].

2.5 Method of Presenting the Discharge Coefficient

For all standardized primary elements, numerous test points have been used to develop an empirical equation that predicts the discharge coefficient from bore and pipe diameter measurements. The accuracy of these equations is usually acceptable, and a flow calibration is seldom performed. However, for Reynolds number, pipe size, etc., outside the specified range of the equation, a signature curve should be used to obtain the discharge coefficient.

In the turbulent flow regime ($Re_D > 4000$), the discharge coefficient for all primary elements can be expressed with an equation of the general form

$$C = C_\infty + \frac{b}{Re_D^n} \quad (20)$$

In which C_∞ is the discharge coefficient at an infinite Reynolds number, and b is the Reynolds number correction term.

Depending on the primary element, the infinite Reynolds number discharge coefficient may be a constant or a function of measured dimensions or tap location. The value of b may also be a function of dimensions, or it may be 0. The Reynolds number exponent n is constant and depending on the primary element.

Therefore by taking in account the discharge coefficient factor, the equation (10) can be written as

$$u_0 = \frac{C_0}{\sqrt{1-\beta^4}} \sqrt{\frac{2(p_a - p_b)}{\rho}} \quad (21)$$

The small effects of kinetic energy factors α_a, α_b are also taken into account in the definition C_0 .

3. Simulation and numerical method

Computational Fluid Dynamics (CFD) is one of the branches of fluid mechanics that uses numerical methods and algorithms to solve and analyze problems that involve fluid flows.

The fundamental basis of any CFD problem is the Navier-Stokes equations, which define any single phase fluid flow. These equations can be simplified by removing terms describing viscosity to yield the Euler equations. Further simplification, by removing terms describing vorticity yields the Full Potential equations. Finally, these equations can be linearized to yield the Linearized Potential equations.

The most fundamental consideration in CFD is how one treats a continuous fluid in a discretized fashion on a computer. One method is to discretize

the spatial domain into small cells to form a volume mesh or grid, and then apply a suitable algorithm to solve the equations of motion (Euler equations for inviscid and Navier-Stokes equations for viscous flow). In addition, such a mesh can be either irregular (for instance consisting of triangles in 2D, or pyramidal solids in 3D) or regular.

In all of these approaches the same basic procedure is followed:

1. The geometry (physical bounds) of the problem is defined.
2. The volume occupied by the fluid is divided into discrete cells (the mesh).
3. The physical modeling is defined - for example, the equations of motions + enthalpy + species conservation.
4. Boundary conditions are defined. This involves specifying the fluid behavior and properties at the boundaries of the problem. For transient problems, the initial conditions are also defined.
5. The equations are solved iteratively as a steady-state or transient.
6. Analysis and visualization of the resulting solution.

The model development and simulation were based on commercial CFD software, Fluent 6.0, and meshing software Gambit 2.0.

The software code is based on the finite volume method on a collocated grid.

Finite volume method is the "classical" or standard approach used most often in commercial software and research codes. The governing equations are solved on discrete control volumes. This integral approach yields a method that is inherently conservative (i.e., quantities such as density remain physically meaningful):

$$\frac{\partial}{\partial t} \iiint Q dV + \iint F dA = 0 \quad (22)$$

Where Q is the vector of conserved variables, F is the vector of fluxes (Euler equations or Navier-Stokes equations), V is the cell volume, and A is the cell surface area [6].

The Fluent 6.0, which is a finite volume code, was used in velocity, pressure and vena contraction computations while Gambit 2.0 provided complete mesh flexibility in solving flow problems with both structured and unstructured meshes in this study. All functions required to compute a solution and display the result in Fluent software are accessible either through an interactive interface or by constructing user-defined-functions (UDS).

The use of CFD simulation usually includes three steps: preprocessing, processing and post processing. In the preprocessing step, a specific system is identified. The geometry and material

properties should be clearly defined. Meshing usually follows after geometry is determined. This is accomplished by dividing geometry into many small elements or volumes. Meshing is complicated work, as it is critical for both the accuracy of final result and the cost of numerical calculation. The setting of boundary conditions, initial conditions and convergence criteria are also completed in preprocessing stage.

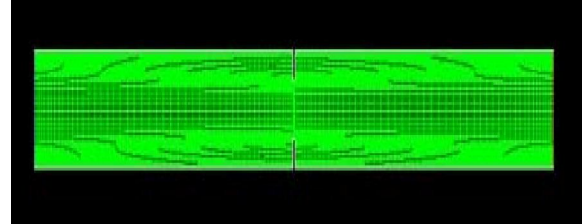


Figure 3. Overall pipe mesh

In the processing stage, the iterative calculations in each cell are carried out until convergence criteria are met. This calculation intensive process constitutes the core content of CFD application. After the completion of processing, the result can be evaluated either numerically or graphically. The graphical methods provide a more convenient way to evaluate the overall effect. This includes vector plot, contour plot, plot of scalar variables, etc. these visualization tools in post processing stage allows quick assessment and comparison of calculation results.

The studied orifice plate is shown in figure 2. The meshing work for the geometry of orifice plate and pipe was done with Gambit® 2.0. Altogether 6358 nodes representing 6298 cells and 12655 faces were used for meshing. Grid refinement was performed according to the concentration gradient within the module geometry.

For both single phase and two phase flow simulation, the flow is assumed to be turbulent and the $k-\varepsilon$ turbulence model is employed. For two-phase model the mixture

Model is used, which is simplified multiphase model and can be used to model inhomogeneous multiphase flows where the phases move at different velocities or homogeneous multiphase flows with phases moving at same velocity. In the multiphase fluid, the fluid contains 90 percent of Methane gas and 10 percent of water liquid.

The distance before and after the orifice, in order to have a fully developed regime flow is $8D$ [7].

The pressure was read before and after the orifice plate, in D and $D/2$ centimeters respectively, and the velocity was read at the center point of the

orifice. The fluids enter the pipe at different Reynolds numbers but at a constant temperature of 300 K, and the walls are assumed to be adiabatic, so they will have no affect on the temperature of the fluid.

4. Results and discussion:

Figure 3 shows the mesh of the computational domain of the overall pipe, and the orifice plate mesh is shown in Figure 4.

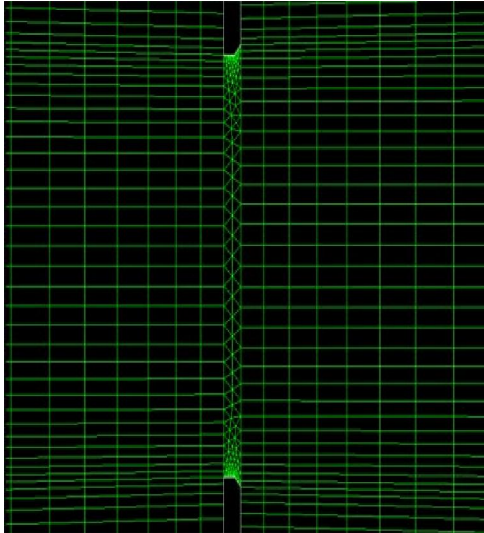


Figure 4. Orifice plate mesh

The results for different β ratios can be seen in the following tables and charts. We have to note that the results were compared by the data available in the “Flow measurement and instrumentation” handbook.

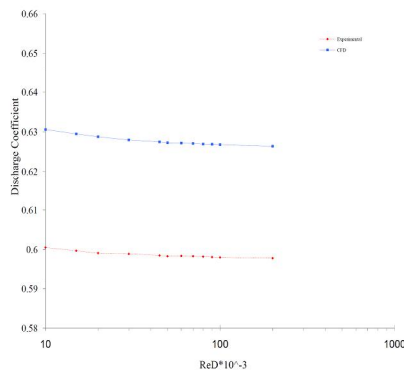


Figure 5. Comparison between experimental and computational calculated discharge coefficient for $\beta = 0.25$.

The results can be seen both as chart and table. The maximum error in this case is 5.012% that decreases while the Pipe’s Reynolds number increases and reaches to 4.784% which is absolutely acceptable.

Table 1. Comparison between experimental and computational calculated discharge coefficient for $\beta = 0.25$.

$Re_D \times 10^{-3}$	C (Exp)	C (CFD)	Error %
10	0.6005	0.6306	5.012
15	0.5997	0.6295	4.969
20	0.5991	0.6288	4.957
30	0.5989	0.628	4.859
45	0.5985	0.6275	4.859
50	0.5983	0.62728	4.843
60	0.5984	0.6272	4.812
70	0.5983	0.6271	4.813
80	0.5982	0.62695	4.806
90	0.5981	0.6269	4.815
100	0.598	0.6268	4.816
200	0.5978	0.6264	4.784

The formula calculated for this case is in the form of a MMF equation

$$C = \frac{a.b + e.Re_D^d}{b + Re_D^d} \quad \therefore$$

$$\begin{cases} a = 0.62549831 \\ b = 0.37210664 \\ e = 0.64120728 \\ d = -0.75425157 \end{cases} \quad (23)$$

With the use of this equation the discharge coefficient can be determined for any Reynolds number for example 53.38×10^{-3} , which was not possible before this.

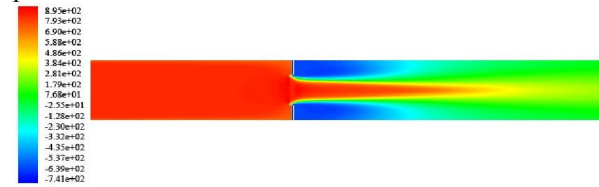


Figure 6. Pressure profile by means of CFD for $\beta = 0.5$

The results can be seen both as chart and table. The maximum error in this case is 5.008% that decreases while the Pipe’s Reynolds number increases and reaches to 3.523% which is absolutely acceptable.

Table 2. Comparison between experimental and computational calculated discharge coefficient for $\beta = 0.5$.

$Re_D \times 10^{-3}$	C (Exp)	C (CFD)	Error %
10	0.619	0.65	5.00
15	0.615	0.6445	4.79
20	0.6125	0.6408	4.62
30	0.61	0.6359	4.24
45	0.6085	0.6327	3.97
50	0.6078	0.6306	3.75
60	0.607	0.6292	3.65
70	0.6065	0.6286	3.64
80	0.6062	0.6282	3.62
90	0.606	0.6278	3.59
100	0.6056	0.6275	3.61
200	0.6045	0.6258	3.52

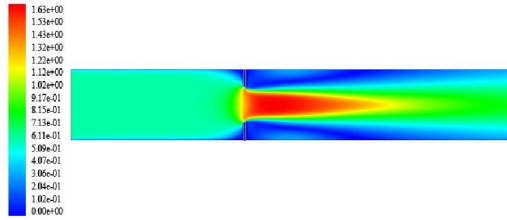


Figure 7. Velocity profile by means of CFD for $\beta=0.5$

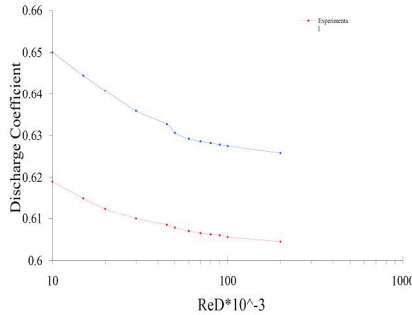


Figure 8. Comparison between experimental and computational calculated discharge coefficient for $\beta=0.5$.

The formula derived for this case is again in the form of a MMF equation:

$$C = \frac{ab + e \cdot Re_D^d}{b + Re_D^d} \quad \therefore \quad \begin{cases} a = 0.6227338 \\ b = 0.32695237 \\ e = 0.72014193 \\ d = -0.88352312 \end{cases} \quad (24)$$

Now by the use of mathematical methods and neural networking, we can determine an equation that can be applied over the range of $0.25 \leq \beta \leq 0.5$ and $10,000 \leq Re_D \leq 200,000$.

$$C = \left[\frac{ab + e \cdot Re_D^d}{b + Re_D^d} \right] \times \sqrt{1 - \beta^4} \quad \therefore \quad \begin{cases} a = 0.62415685 \\ b = 0.30651715 \\ e = 0.67147866 \\ d = -0.86214300 \end{cases} \quad (25)$$

The maximum error for equation 42 is assumed to be 7%. We have to note that the error will decrease while the Reynolds number increases. Using

equation 42 for $\beta=0.35$ as an example, will result as in given in table 3:

Table 2. Comparison between the experimental and the determined discharge coefficient

$Re_D \times 10^{-3}$	C (Exp)	C (CFD)	Error %
10	0.606	0.633	4.45
15	0.6041	0.6307	4.40
20	0.6034	0.6287	4.19
30	0.602	0.6264	4.05
45	0.6018	0.6245	3.77
50	0.6016	0.6241	3.74
60	0.6015	0.6235	3.65
70	0.6015	0.6230	3.57
80	0.6013	0.6227	3.56
90	0.6012	0.6224	3.52
100	0.6008	0.6221	3.54
200	0.600	0.6209	3.48

5. Conclusion:

The objective of this research was to simulate the blood flow over the range of $0.25 \leq \beta \leq 0.5$ and $10,000 \leq Re_D \leq 200,000$. The correlation was achieved through numerical methods using Fluent 6.0 software and is expressed as a function of the pipe's Reynolds number and the β ratio. As a result, each one of these non-ideal mechanisms can be analyzed independently from the influence of the other mechanisms.

Corresponding Author:

Ameneh Langari
North Khorasan University of Medical Sciences,
Bojnurd, Iran
E-mail: amenehlangari@yahoo.com

References:

1. Netanel Korin et al., Shear-Activated Nanotherapeutics for Drug Targeting to Obstructed Blood Vessels, *Science*, 2012, DOI: 10.1126/science.1217815
2. ASME 3M. Differential producers used for measurement of fluids in pipes (orifices, nozzle, nozzle venturi, venturi). ASME, New York, 1985
3. ANSI/API 2530. Orifice metering of natural gas, American gas association, New York, 1985
4. McCabe, Smith, Harriot, Unit operations of chemical engineering. McGraw-Hill 2001; 15:729-736.
5. Hewitt G F. Measurements of two phase flow parameters. Academic, London, 1978.
6. Cao Z, Wiley D E, Fane A G. CFD simulations of net-type turbulence promoters in a narrow channel. *J. Membr. Sci.* 2001; 185()
7. ANSI/ASME MFC-2M, Measurement uncertainty for fluid flow in closed conduits. ANSI, New York, 1988.
8. Johnson RC. Calculations of real gas effects in flow through critical flow nozzles. *ASME J Basic Eng Series D* 1964; 86:519-26.